Davydov model: The quantum, mixed quantum-classical, and full classical systems

Leonor Cruzeiro-Hansson[1] and Shozo Takeno[2]
[1]*Crystallography Department, Birkbeck College, Malet Street, London WC1E 7HX, United Kingdom*
[2]*Department of Information Systems, Faculty of Information Science, Osaka Institute of Technology, 1-79-1 Kitayama, Hirakata, Osaka 573-01, Japan*
(Received 23 December 1996)

The need for a mechanism for energy transfer in proteins, such as the Davydov model, is emphasized. Here we concentrate on the finite-temperature properties of the Davydov model in three regimes: the quantum regime, in which both the excitation and the lattice are treated quantum mechanically; the mixed quantum-classical regime, in which the excitation is treated quantum mechanically but the lattice is considered classical; and the classical regime, in which both the excitation and the lattice are treated classically. The equilibrium behavior can be determined exactly in the three regimes and thus provides a way to evaluate the validity of the latter two regimes as well as a reference point for the nonequilibrium studies. Our results indicate that while at low temperature both the classical and the semiclassical regimes differ from the full quantum Davydov system, at biological temperatures the mixed quantum-classical regime leads to the same equilibrium behavior as the full quantum Davydov system. The nonequilibrium properties in the mixed quantum-classical regime are studied with a different set of equations of motion for finite temperature, which are derived in great detail in Sec. VI. At biological temperatures, these equations predict that the Davydov soliton is unstable. However, the states populated at biological temperatures preserve one of the features of the Davydov soliton, namely, the localization of the amide I excitation. The nonequilibrium equations in Sec. VI lead to a Brownian-like motion of the amide I excitation from the active site to other regions of the protein. This stochastic mechanism for energy transfer may constitute a first step in many biological processes. [S1063-651X(97)09207-6]

PACS number(s): 87.15.−v, 05.40.+j, 71.38.+i

I. INTRODUCTION

A central aspect of many biological processes, such as muscle contraction, active transport, protein folding, and DNA repair, is the transduction of the energy released in the chemical reaction of the hydrolysis of adenosinetriphosphate (ATP) into work. The transduction is known to involve conformational changes of the proteins that perform the work but, although in some cases the final conformation has been determined, the mechanism by which such conformational changes take place is not known. The usual biological view is to assume that the chemical reaction can trigger the conformational change in the same direct way in which a part in a macroscopic machine responds to a macroscopic kick. However, a chemical reaction is a localized process, involving only a small amount of atoms in a protein, and cannot directly impart the collective momenta and/or angular momenta that lead to the observed conformational changes. What the triggers of the protein function can and very probably do is create local excitations in the proteins. The processes by which these initial excitations lead to the conformational changes and thereby to the work produced by biological systems is at the moment largely not understood.

While a complete protein work cycle can last from microseconds to milliseconds or more, the model proposed by Davydov [1] describes what happens to the energy released in the picosecond to nanosecond time scale after the chemical reaction. One basic assumption of the Davydov model is that the energy released in the hydrolysis of ATP is initially stored in a particular mode of the protein peptide groups, called amide I. The Davydov model describes the interaction of the amide I vibrations with the hydrogen bonds that stabilize the α helix [1].

Davydov's Hamiltonian is formally similar to the Fröhlich-Holstein Hamiltonian for the interaction of electrons with a polarizable lattice. Thus the Hamiltonian $\hat{H}$ is

$$\hat{H}=\hat{H}_{\rm qp}+\hat{H}_{\rm ph}+\hat{H}_{\rm int}, \tag{1}$$

where $\hat{H}_{\rm qp}$ is the quasiparticle Hamiltonian, which describes the motion of the amide I excitations between adjacent sites; $\hat{H}_{\rm ph}$ is the phonon Hamiltonian, which describes the vibrations of the lattice; and $\hat{H}_{\rm int}$ is the interaction Hamiltonian, which describes the interaction of the amide I excitation with the lattice. The quasiparticle Hamiltonian $\hat{H}_{\rm qp}$ is

$$\hat{H}_{\rm qp}=\epsilon\sum_{n=1}^{N}\hat{A}_n^{\dagger}\hat{A}_n-V\sum_{n=1}^{N}[(\hat{A}_n^{\dagger}\hat{A}_{n-1}+\hat{A}_n^{\dagger}\hat{A}_{n+1})], \tag{2}$$

where ϵ is the energy of the amide I vibration, $-V$ is the dipole-dipole interaction energy of the amide I excitations in neighboring sites, $\hat{A}_n^{\dagger}$ ($\hat{A}_n$) is the boson creation (annihilation) operator for a quasiparticle at site n, and N is the number of peptide groups in the lattice. The phonon Hamiltonian $\hat{H}_{\rm ph}$ is

$$\hat{H}_{\rm ph}=\tfrac{1}{2}\sum_{n=1}^{N}\left[\kappa(\hat{U}_n-\hat{U}_{n-1})^2+\frac{\hat{P}_n^2}{M}\right], \tag{3}$$

 © 1997 The American Physical Society

where $\hat{u}_n$ is the displacement operator from the equilibrium position of site n, $\hat{P}_n$ is the momentum operator of site n, M is the mass of each peptide group, and κ is the elasticity constant of the lattice. Finally, the interaction Hamiltonian $\hat{H}_{\rm int}$ is

$$\hat{H}_{\rm int}=\chi\sum_{n=1}^{N}[(\hat{U}_{n+1}-\hat{U}_{n-1})\hat{A}_n^{\dagger}\hat{A}_n], \tag{4}$$

where χ is an anharmonic parameter arising from the coupling between the quasiparticle and the lattice displacements.

The Davydov model has been the object of many theoretical studies [2] and it continues to attract the attention of many researchers [3–7]. Here three regimes will be considered: the *quantum* theory, in which both the amide I vibration and the lattice site motion are treated quantum mechanically; the *mixed quantum-classical* theory, in which the amide I vibration is treated quantum mechanically but the lattice is classical; and the *classical* theory, in which both the amide I and the lattice motions are treated classically [8]. While in previous studies the aim has been to determine exact solutions of the quantum Davydov system [3,4] or to establish the range of validity of the mixed quantum-classical system [5], this paper concentrates on the finite-temperature properties of the Davydov model in the three regimes. As it will be shown, it is possible to find, by numerical simulations, the equilibrium behavior of the Davydov system in the three regimes. The importance of these studies is that the equilibrium behavior provides a reference point for the nonequilibrium studies, for which exact behavior can only be determined in the classical regime. Equilibrium averages do not suffer from the effect of approximations, either in the form of the wave functions or in the derivation of the equations. On the other hand, the integration of nonequilibrium equations for sufficiently long times should lead to an equilibrium ensemble. Thus, comparing long-term nonequilibrium dynamical simulations with equilibrium averages obtained by independent Monte Carlo simulations constitutes one way of evaluating the accuracy of the dynamical equations. One of the aims of this paper is the justification of a system of equations that has been proposed before [9,10] [cf. Eqs. (28) and (29) in Sec. VI] to describe the equilibrium behavior of the mixed quantum-classical Davydov system.

The paper is organized as follows. In Secs. II, III, and IV the equilibrium behavior of the quantum, mixed quantum-classical, and classical Davydov systems, respectively, is examined. Section V deals with the nonequilibrium situation of the classical Davydov system. In Sec. VI a different system of equations to describe the nonequilibrium situation of the mixed quantum-classical Davydov system is introduced and its validity and possible limitations are assessed. Section VII summarizes and discusses the main results. Finally, the details of the derivation of Eqs. (11)–(14) and of Eq. (30) are given in Appendixes A and B, respectively.

II. EQUILIBRIUM QUANTUM-MECHANICAL THEORY

The equilibrium properties of a quantum system can be determined from the density matrix operator $\hat{\rho}=e^{-\beta\hat{H}}$, where $\beta=1/k_BT$, k_B being the Boltzmann constant and T the absolute temperature. The thermodynamic average of a quantity $\hat{B}(\{\hat{A}_j\},\{\hat{U}_j\},\{\hat{P}_j\})$, given by

$$\langle\langle\hat{B}\rangle\rangle=\frac{\mathrm{Tr}(\epsilon^{-\beta\hat{H}}\hat{B})}{\mathrm{Tr}(e^{-\beta\hat{H}})}, \tag{5}$$

can be determined by quantum Monte Carlo methods. Such simulations have been performed to determine the thermal equilibrium values of quantities such as the lattice deformation correlated with the position of the amide I vibration, to determine the excitation density-density correlation for one excitation state, and to probe multiexcitation states [11].

The basis for the states chosen by Wang, Brown, and Lindenberg [11] is optimal from the point of view of efficiency in the calculation of the observables they were interested in. However, it does not allow for an easy transition from the full quantum to the mixed quantum-classical case. Here a different basis set is considered, namely,

$$|Q\rangle=\prod_{j=1,N}|Q_j\rangle|\psi_n(\{q_j\})\rangle,\quad n=1,\ldots,N, \tag{6}$$

where $|Q_j\rangle$ and $\{q_j\}$ are, respectively, the eigenvectors and eigenvalues of the displacement operators $\hat{U}_j$,

$$\hat{U}_j|Q_j\rangle=q_j|Q_j\rangle, \tag{7}$$

and $|\psi_n(\{q_j\})\rangle$ are the eigenvectors of the operator $\tilde{H}(\{q_j\})$,

$$\hat{H}\prod_{j=1,N}|Q_j\rangle=\tilde{H}(\{q_j\})\prod_{j=1,N}|Q_j\rangle, \tag{8}$$

$$\tilde{H}(\{q_j\})|\psi_n(\{q_j\})\rangle=E_n^T(\{q_j\})|\psi_n(\{q_j\})\rangle. \tag{9}$$

The average of a quantum variable $\hat{B}$ can then be obtained from the expression

$$\langle\langle\hat{B}\rangle\rangle=\frac{\int\prod_{j=1,N}dq_j^0\equiv dq_j^{2L}\sum_{n_0\equiv n_{2L}=1}^{N}\langle\psi_{n_0}|\langle Q_j^0|e^{-\beta\hat{H}}\hat{B}|Q_j^{2L}\rangle|\psi_{n_{2L}}\rangle}{\int\prod_{j=1,N}dq_j^0\equiv dq_j^{2L}\sum_{n_0\equiv n_{2L}=1}^{N}\langle\psi_{n_0}|\langle Q_j^0|e^{-\beta\hat{H}}|Q_j^{2L}\rangle|\psi_{n_{2L}}\rangle}. \tag{10}$$

From Eqs. (8) and (9) it may appear that Eq. (10) is easily simplified by substituting $e^{-\beta E^T_{n_0}(\{q_j^{n_0}\})}$ for $e^{-\beta\hat{H}}$. However, as they stand, Eqs. (8) and (9) are essentially formal expressions in which the dependence of $\widetilde{H}$ on the eigenvalues $\{q_j^0\}$ is not easy to determine because of the kinetic-energy operator for the lattice. In order to determine the matrix elements in Eq. (10) we follow the path-integral approach first proposed by Feynman [12]. As is derived in Appendix A, the following expression for the thermodynamic average is obtained:

$$\langle\langle\hat{B}\rangle\rangle=\frac{\int\cdots\int\prod_{j=1,N}dq_j^1dq_j^2\cdots dq_j^L\mathcal{D}(\{q_j^s\})\sum_{n_1,n_1,\ldots,n_L=1}^{N}\mathcal{B}(\{q_j^s\})}{\int\cdots\int\prod_{j=1,N}dq_j^1dq_j^2\cdots dq_j^L\mathcal{D}(\{q_j^s\})\sum_{n_1,n_2,\ldots,n_L=1}^{N}\mathcal{F}(\{q_j^s\})},\tag{11}$$

where

$$\mathcal{D}=\exp\left(-\frac{1}{2\lambda^2}\sum_{s=1}^{L}\sum_{j=1}^{N}(q_j^s-q_j^{s-1})^2\right)\times\exp\left(-\frac{\tau}{2}\kappa\sum_{s=1}^{L}\sum_{j=1}^{N}(q_j^s-q_{j-1}^s)^2\right),\tag{12}$$

$$\mathcal{B}=\sum_{n_1,n_2,\ldots,n_{L=1}}^{N}e^{-\tau(E_{n_1}+E_{n_2}+\cdots+E_{n_L})}\langle\psi_{n_L}|\psi_{n_1}\rangle\langle\psi_{n_1}|\psi_{n_2}\rangle\cdots\langle\psi_{n_{L-2}}|\psi_{n_{L-1}}\rangle\langle\psi_{n_{L-1}}|\hat{B}|\psi_{N_L}\rangle,\tag{13}$$

$$\mathcal{F}=\sum_{n_1,n_2,\ldots,n_{L=1}}^{N}e^{-\tau(E_{n_1}+E_{n_2}+\cdots+E_{n_L})}\langle\psi_{n_L}|\psi_{n_1}\rangle\langle\psi_{n_1}|\psi_{n_2}\rangle\cdots\langle\psi_{n_{L-2}}|\psi_{n_{L-1}}\rangle\langle\psi_{n_{L-1}}|\psi_{n_L}\rangle.\tag{14}$$

Expression (11) can be calculated by classical Monte Carlo methods. Indeed, taking $\mathcal{D}$ to be a distribution function, the Metropolis scheme [13] can be used to sample the space spanned by $\{q_j^s\}$. To calculate the thermal average of $\hat{B}$ at a temperature T following the latter expression it is necessary to calculate the ensemble average of $\mathcal{B}$ and divide it by the ensemble average of $\mathcal{F}$.

Although less efficient than the expressions used by Wang, Brown, and Lindenberg [11], Eqs. (11)–(14) are completely general. They show that the only theoretical impediment to the study of the equilibrium properties of the full quantum Davydov system is the availability of fast computers. Indeed, the dimension of the configuration space to be sampled is LN, where L must be large enough for the Trotter formula [Eq. (A2)] to be valid. As the temperature decreases, to maintain the same accuracy, increasingly larger values of L are necessary. In practice, the value of L can be determined by following the convergence of the results of simulations made with different values of L. This is analogous to the way in which the accuracy of a numerical integration of differential equations can be checked by comparing the results obtained with increasingly small time steps. Wang, Brown, and Lindenberg's simulations [11] can thus be regarded as exact results for the full quantum Davydov model at thermal equilibrium and constitute an accurate reference for the nonequilibrium, finite-temperature behavior of the quantum Davydov system. They showed that at low temperature the amide I vibration is in a state very similar to that of a small polaron, occupying an average of five sites. As temperature increases, the width of the state *decreases* and at biological temperatures the amide I vibration is essentially localized in one site.

III. EQUILIBRIUM MIXED QUANTUM-CLASSICAL THEORY

The mixed quantum-classical case corresponds to treating the lattice oscillators classically. In this case, the displacements $\{u_j\}$ and momenta $\{p_j\}$ in the Hamiltonian (1)–(4) are c numbers [8]. The sum over s in Eq. (12), which reflects the quantum delocalization of the lattice sites, is reduced to one term corresponding to the point at which the sites are localized and the average of a quantity $\hat{B}(\{\hat{A}_j\},\{u_j\},\{p_j\})$ becomes

$$\langle\langle\hat{B}\rangle\rangle=\frac{\int\prod_{j=1}^{N}du_j\mathcal{D}_{\rm qc}(\{u_j\})\mathcal{B}_{\rm qc}(\{u_j\})}{\int\prod_{j=1}^{N}du_j\mathcal{D}_{\rm qc}(\{u_j\})\mathcal{F}_{\rm qc}(\{u_j\})},\tag{15}$$

where distribution $\mathcal{D}_{\rm qc}$ is

$$\mathcal{D}_{\rm qc}=\exp\left(-\frac{\beta}{2}\kappa\sum_{j=1}^{N}(u_j-u_{j-1})^2\right),\tag{16}$$

$\mathcal{B}_{\rm qc}$ and $\mathcal{F}_{\rm qc}$ are

$$\mathcal{B}_{\rm qc}=\sum_{n=1}^{N}e^{-\beta E_n}\langle\psi_n|\hat{B}|\psi_n\rangle,\tag{17}$$

$$\mathcal{F}_{\rm qc}=\sum_{n=1}^{N}e^{-\beta E_n},\tag{18}$$

and E_n is

$$(\hat{H}_{\rm qp}+\hat{H}_{\rm int})|\psi_n(\{u_j\})\rangle=E_n(\{u_j\})|\psi_n(\{u_j\})\rangle.\tag{19}$$

Equations (15)–(19) can also be derived by noticing that in the absence of the kinetic energy for the lattice they coincide with the average (10) for the quantum system. Neglecting the kinetic energy of the lattice corresponds to making the adiabatic approximation, which has been used by many authors. However, it should be pointed out that, in general, the adiabatic approximation represents a restriction *within* the mixed quantum-classical system and leads to a reduced class of dynamical trajectories. It is only in the context of thermodynamic averages, which for classical systems do not depend on the masses and velocities of the particles, that the adiabatic approximation is equivalent to the assumption that the lattice is classical.

The derivation of Eqs. (15)–(19) above shows that the mixed quantum-classical regime is valid when $\lambda^2 \rightarrow 0$, in which case the Gaussian distribution in Eq. (12), which accounts for the quantum delocalization of the lattice sites, becomes a δ function, representing a completely localized lattice site. Indeed, λ^2 is a measure of the uncertainty in the position of the lattice oscillators and as this uncertainty is reduced the behavior of the oscillators becomes more classical. An estimate of the value of the temperature above which the mixed quantum-classical Davydov model is valid can be obtained by comparing the quantum uncertainty λ^2 with the thermal uncertainty. In a first-order approximation this corresponds to comparing the importance of the first exponential in Eq. (12) with that of the second exponential. When the quantum uncertainty of the lattice is smaller than the thermal uncertainty the lattice can be considered to be classical. The thermal uncertainty for a harmonic oscillator is $k_B T/\kappa$ and thus for temperatures T above $(\hbar/k_B)\sqrt{\kappa/M}$ the quantum effects in the lattice can be neglected. For the α-helix parameters [2] the critical temperature is 60 K. The Davydov system, however, is not a harmonic oscillator, but N harmonic oscillators coupled to a quantum quasiparticle. Comparisons of the lattice displacement correlated with the excitation in the full quantum and in the mixed quantum-classical case showed that quantum effects can be neglected for $T > 11$ K [14].

The most efficient way of evaluating the mixed quantum-classical average (15)–(19) is similar to that already described for the full quantum case, i.e., the displacements can be sampled with the distribution $\mathcal{D}_{\rm qc}$ and the averages of the quantities $\mathcal{B}_{\rm qc}$ and $\mathcal{F}_{\rm qc}$ can be calculated from the configurations accepted. Another way of calculating the average is to use the Metropolis scheme also to select states $\langle \psi_n |$ with the probability $e^{-\beta E_n}$ and for each value of the displacements take only one term $\langle \psi_n | \hat{B} | \psi_n \rangle$ instead of evaluating the sum over all states n in $\mathcal{B}_{\rm qc}$ [Eq. (17)]. This would be much less efficient than calculating the sum over n in $\mathcal{B}_{\rm qc}$, but for a sufficiently large number of conformations $\{u_j\}$ of the lattice it would lead to the same ensemble. This latter way of evaluating the thermodynamic averages in the mixed quantum-classical case bears a strong resemblance to the way in which the corresponding nonequilibrium case is described by Eqs. (28) and (29) in Sec. VI below.

IV. EQUILIBRIUM CLASSICAL THEORY

In the full classical case, not only the displacements and momenta but also the quasiparticle operators for the amide I excitation $\{a_j\}$ are c numbers. It is easy to see that in this case the thermodynamic average of a quantity $B(\{a_j\},\{u_j\})$ is

$$\langle\langle B \rangle\rangle = \frac{\displaystyle\int_{2N \text{ unit sphere}} \{da_n^r\}\{da_n^i\} \int \{du_n\} e^{-\beta H(\{a_n^r\},\{a_n^i\},\{u_n\})} B(\{a_n^r\},\{a_n^i\},\{u_n\})}{\displaystyle\int_{2N \text{ unit sphere}} \{da_n^r\}\{da_n^i\} \int \{du_n\} e^{-\beta H(\{a_n^r\},\{a_n^i\},\{u_n\})}}, \tag{20}$$

where a_n^r and a_n^i are, respectively, the real and imaginary parts of the classical complex amplitude a_n of the amide I vibration in site n.

In a previous publication, this expression was used to study the mechanism of thermal destabilization of the Davydov soliton [15] in a regime mistakenly called semiclassical. It was found that the Davydov soliton did not decay into excitons and that at high temperatures a parameter-independent behavior sets in. This, however, applies only in the full classical case.

It has been shown before that at biological temperatures, while in the classical Davydov system the average state of the amide I vibration is delocalized, the corresponding average state in the mixed quantum-classical system is highly localized [9]. It should also be pointed out that this localized state does *not* coincide with the Davydov soliton because the lattice contraction associated with it is much smaller than the lattice distortions induced by thermal agitation.

The differences between the mixed quantum-classical and the full classical Davydov systems are also illustrated in Fig. 1, where one observable, namely, the absorption spectrum associated with the amide I vibration, is displayed. The solid line is for the mixed quantum-classical and the dashed line is for the full classical regime. An immediate observation is that the mixed quantum-classical line is much broader than the full classical line. Indeed, a Gaussian fit of the lines yields a standard deviation of 44 cm^{-1} for the mixed quantum-classical case and a standard deviation of 1 cm^{-1} for the full classical case. The width of the absorption spectrum in the mixed quantum-classical Davydov system is due to inhomogeneous broadening, i.e., the averaging over the different quantum states associated with each lattice conformation specified by $\{u_j\}$, $j = 1,N$ [cf. Eqs. (15)–(19)]. Another important difference between the mixed quantum-classical and the classical spectrum is the shift with respect to the isolated amide I excitation energy of 1660 cm^{-1}.

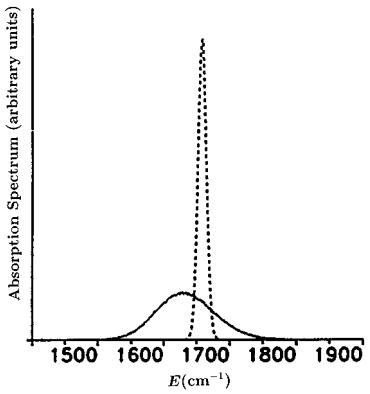

FIG. 1. Absorption spectrum predicted by the mixed quantum-classical (solid line) and the fully classical (dashed line) Davydov systems. The parameters are $V=1.55\times10^{-22}$ J, $\kappa=39$ N/m, $\chi=62$ pN, and $T=310$ K.

While in the mixed quantum-classical case this shift is approximately $-27\ \mathrm{cm}^{-1}$, for the full classical case it is also negative, but less than $0.01\ \mathrm{cm}^{-1}$ in absolute terms. The larger frequency shift in the mixed quantum-classical Davydov system is due to the fact that the strongly localized amide I excitation leads to a greater lattice distortion correlated with the position of the excitation and the greater the distortion, the greater the frequency shift. It is interesting to note that, at low temperatures, the full quantum Davydov system leads to a lattice distortion *greater* than the mixed quantum-classical system and thus will have a lower energy [14].

Although the equilibrium results mentioned up to now cannot provide dynamical information, they are very important because, as already emphasized in the Introduction, they constitute an essential reference for the nonequilibrium studies, i.e., the dynamical trajectories must not contradict what is known from equilibrium studies. These equilibrium references for the nonequilibrium behavior of the Davydov system in the three regimes can be determined with any desired accuracy by numerical simulations.

The fact that the equilibrium Monte Carlo simulations of the full quantum and of the mixed quantum-classical system indicate that the average states of the amide I excitation are localized at biological temperatures [9–11,14] means that localized states have an infinite lifetime. That is, if they are localized at equilibrium, which is equivalent to integrating the equations of motion for a very long time, they are thermally stable. Thus, in this case, the equilibrium Monte Carlo simulations can even give an estimate for the lifetime of the localized states.

V. NONEQUILIBRIUM CLASSICAL THEORY

The previous sections dealt with the thermal equilibrium properties of the Davydov system in the three regimes. Thermal equilibrium, however, corresponds to the behavior after very long times and the motion of the amide I vibration in a protein is a short, transient process. While the equilibrium studies tell us that the Davydov soliton is unstable at biological temperatures, they cannot tell us how long it lasts if it happens to be created by the hydrolysis of ATP. For the temporal evolution it is necessary to resort to the equations of motion. For the full classical case, in which u_j and p_j, and a_j and $i\hbar a_j^*$, respectively, are canonically conjugate variables, the equations of motion are easily derived from Hamilton equations

$$i\hbar\,\frac{da_n}{dt}=\epsilon a_n-V(a_{n-1}+a_{n+1})+\chi(u_{n+1}-u_{n-1})a_n, \tag{21}$$

$$M\,\frac{d^2u_n}{dt^2}=\chi(|a_{n+1}|^2-|a_{n-1}|^2)+\kappa(u_{n+1}+u_{n-1}-2u_n). \tag{22}$$

Continuous and adiabatic approximations of these equations have been studied by Davydov and co-workers [1] and extended versions were simulated numerically by Scott and co-workers [16]. A central finding is that for a fixed energy level and above a threshold for the nonlinearity χ, a soliton solution forms, which propagates without dispersion along the lattice. It is also known that the evolution of the excitation depends not only on the energy level but also on the phase of the initial condition [17] and like many other nonlinear systems also this one can have chaotic behavior [18].

To study the motion of the amide I excitation and its associated lattice displacements at finite temperature Lomdahl and Kerr [19] used the equations

$$i\hbar\,\frac{da_n}{dt}=\epsilon a_n-V(a_{n-1}+a_{n+1})+\chi(u_{n+1}-u_{n-1})a_n, \tag{23}$$

$$M\,\frac{d^2u_n}{dt^2}=\chi(|a_{n+1}|^2-|a_{n-1}|^2)+\kappa(u_{n+1}+u_{n-1}-2u_n)+F_n(t)-\Gamma\,\frac{du_n}{dt}, \tag{24}$$

which are obtained by adding the stochastic forces $F_n(t)$ and the friction terms $-\Gamma(du_n/dt)$ to Eq. (22). When the latter two terms obey the fluctuation-dissipation relation $\langle F_n(t)F_m(t')\rangle=2M\Gamma k_BT\delta_{nm}\delta(t-t')$, it has been proved that such a thermalization scheme applied to a classical system leads to the canonical ensemble for that classical system [20]. Lomdahl and Kerr, however, aimed at describing the finite-temperature motion of the amide I excitation in the full quantum case. They found that the equations (23) and (24) lead to the dispersion of the Davydov soliton in a few picoseconds [19]. A more systematic work by Förner showed defined ranges of parameters in which the excitation stays localized at biological temperatures [21]. However, both studies pertain to the nonequilibrium behavior of a *classical* amide I excitation in a classical lattice.

VI. NONEQUILIBRIUM MIXED QUANTUM-CLASSICAL THEORY

A general solution for the one quantum state of the mixed quantum-classical Davydov system is [22]

$$|\psi\rangle=\sum_{j=1}^{N}\varphi_j(\{u_n\},\{p_n\},t)\hat{A}_j^{\dagger}|0\rangle, \tag{25}$$

where φ_j is the probability amplitude for an excitation in site j and the dependence of φ_j on the displacements and momenta of the lattice are not specified *a priori*. Inserting Eq. (25) in the Schrödinger equation for the mixed quantum-classical Davydov system and using the Hamilton equations for the lattice variables, the following equations of motion are derived:

$$\imath\hbar \frac{d\varphi_n}{dt} = \epsilon\varphi_n - V(\varphi_{n-1}+\varphi_{n+1}) + \chi(u_{n+1}-u_{n-1})\varphi_n, \tag{26}$$

$$M \frac{d^2u_n}{dt^2} = \chi(|\varphi_{n+1}|^2 - |\varphi_{n-1}|^2) + \kappa(u_{n+1}+u_{n-1}-2u_n). \tag{27}$$

The formal identity of the above equations of motion with those of the fully classical system (21) and (22) is immediately apparent. However, it should be remembered that while in the classical equation (21) the variables a_n represent classical complex amplitudes and any quantity $B(\{a_j\},\{u_j\},\{p_j\})$ can be readily calculated, in the mixed quantum-classical system, $\{\varphi_n\}$ are probability amplitudes and the corresponding quantity must be calculated as $\mathcal{B}(\{\varphi_j\},\{u_j\},\{p_j\}) = \langle\psi|\hat{B}|\psi\rangle$. In general, the functional dependence of $\mathcal{B}$ on the probability amplitudes is not the same as the functional dependence of B on the complex amplitudes. Any quantity B whose functional dependence on a_n is the same as that of $\mathcal{B}$ on $\{\varphi_j\}$ will have the same values in the two systems. One of these quantities is the energy.

How can we extend Eqs. (26) and (27) in order to include a coupling to a thermal bath that preserves the quantum character of the amide I vibration? Lomdahl and Kerr reasoned that since at biological temperatures the Boltzmann distribution is a very good approximation of the Bose distribution for the lattice, it should be possible to couple the lattice to a classical bath. However, as mentioned above, this leads to a classical treatment of the amide I excitation as well. The problem arises when any mixed quantum-classical system is coupled to a classical bath and has also been addressed by other authors [23,24]. In the case of the Davydov system a comparison of the averages obtained by Monte Carlo simulations of the fully classical system [cf. Eq. (20)] and the classical Langevin equations (23) and (24) showed that they were equal [25]. *A fortiori* it is easy to understand that a classical scheme to thermalize a system represented by equations that are formally identical to that of a fully classical counterpart should lead to the canonical ensemble of the fully classical system. The Langevin terms are known to generate the correct canonical ensemble for classical systems [20] and nothing in Eqs. (26) and (27) above indicates that φ_j are probability amplitudes for which random superpositions should cancel each other out. Just as the stochastic and damping terms are made to obey the fluctuation-dissipation theorem, there should also be a constraint on the variables φ_j that would ensure that quantum statistics would apply in their case. These would-be exact, finite-temperature, equations of motion for the mixed system are not available. Other authors have added constraints that either push the states back to eigenstates [23] or push the density matrix to its known equilibrium value [24]. These approaches are not easy to apply to more complex systems, such as the Davydov model. Instead, in previous publications the following equations have been proposed [9,10]:

$$E\varphi_n = \epsilon\varphi_n - V(\varphi_{n-1}+\varphi_{n+1}) + \chi(u_{n+1}-u_{n-1})\varphi_n, \tag{28}$$

$$M \frac{d^2u_n}{dt^2} = \chi(|\varphi_{n+1}|^2 - |\varphi_{n-1}|^2) + \kappa(u_{n+1}+u_{n-1}-2u_n) + F_n(t) - \Gamma \frac{du_n}{dt}. \tag{29}$$

The equations are integrated by solving the eigenvalue problem (28) at each time step and applying the Metropolis scheme [13] to choose which energy state E will drive the lattice equation (29) at that time step.

It can be shown that, without the stochastic and random terms, Eqs. (28) and (29) are valid if the quantum quasiparticle is much faster than the lattice. The detailed proof is as follows. The integration of Eq. (27) leads to (see Appendix B for a detailed derivation)

$$\begin{aligned} u_{n+1}-u_{n-1} = &-\frac{\chi}{\kappa}(2|\varphi_n|^2 + |\varphi_{n+1}|^2 + |\varphi_{n-1}|^2) \\ &+ \frac{\chi}{\kappa}\sum_{m=1}^{N}\int_0^t ds\; M_{n-m}(t-s)\left[\frac{d}{ds}|\varphi_m(s)|^2\right] \\ &+ \frac{\chi}{\kappa}\sum_{m=1}^{N}\int_0^t ds\; M_{n-m}(t-s)|\varphi_m(0)|^2 + f_{n+1} \\ &- f_{n-1}, \end{aligned} \tag{30}$$

where

$$M_n(t) = 2J_{2n}(\omega_1 t) + J_{2(n+1)}(\omega_1 t) + J_{2(n-1)}(\omega_1 t), \tag{31}$$

$$\omega_1^2 = \frac{4\kappa}{M}, \tag{32}$$

$$\begin{aligned} f_n(t) = \sum_{m=1}^{N}\Big[&J_{2(n-m)}(\omega_1 t)u_m(0) \\ &+ \int ds\; J_{2(n-m)}(\omega_1 t)\dot{u}_m(0)\Big], \end{aligned} \tag{33}$$

and the J's are Bessel functions. Inserting expression (30) into Eq. (26) we obtain

$$\iota\hbar\,\frac{d\varphi_n}{dt}=\epsilon\varphi_n-V(\varphi_{n-1}+\varphi_{n+1})-\frac{\chi^2}{\kappa}\,(2|\varphi_n|^2+|\varphi_{n+1}|^2+|\varphi_{n-1}|^2)\varphi_n+\frac{\chi^2}{\kappa}\left\{\sum_{m=1}^{N}\int_0^t ds\; M_{n-m}(t-s)\times\left[\frac{d}{ds}\,|\varphi_m(s)|^2\right]+\sum_{m=1}^{N} M_{n-m}(t)|\varphi_m(0)|^2\right\}\varphi_n+\frac{\chi^2}{\kappa}\,[f_{n+1}(t)-f_{n-1}(t)]\varphi_n. \tag{34}$$

Equation (34) is completely equivalent to Eqs. (26) and (27). The third term is the source of the self-trapping, the fourth term contains a memory kernel, and the fifth term represents some fluctuations. The restrictions implied by the adiabatic approximation can be clearly identified here since the adiabatic approximation consists in neglecting the memory and fluctuation terms, in which case the discrete self-trapping equation is recovered [26]. Let us now consider solutions of the form

$$\varphi_n(t)=\phi_n(t)e^{-\iota\omega t}. \tag{35}$$

Inserting Eq. (35) into Eq. (34) we get

$$\iota\hbar\left(\frac{d\phi_n}{dt}-\iota\omega\phi_n\right)=\epsilon\phi_n-V(\phi_{n-1}+\phi_{n+1})-\frac{\chi^2}{\kappa}\,(2|\phi_n|^2+|\phi_{n+1}|^2+|\phi_{n-1}|^2)\phi_n+\frac{\chi^2}{\kappa}\left\{\sum_{m=1}^{N}\int_0^t ds\; M_{n-m}(t-s)\times\left[\frac{d}{ds}\,|\phi_m(s)|^2\right]\phi_n+\sum_{m=1}^{N} M_{n-m}(t)|\phi_m(0)|^2\right\}+\frac{\chi^2}{\kappa}\,[f_{n+1}(t)-f_{n-1}(t)]\phi_n. \tag{36}$$

The left-hand side of Eq. (36) is $\iota\hbar(d\phi_n/dt)+E\phi_n$, where $E=\hbar\omega\approx\hbar\epsilon$ and $\hbar(d\phi_n/dt)\approx\hbar\omega_1$, the energy of acoustic phonons. Since $\epsilon\gg\hbar\omega_1$ we have

$$\hbar\,\frac{d\phi_n}{dt}\ll E\phi_n. \tag{37}$$

Using relation (37) in Eq. (36) we get

$$E\phi_n=\epsilon\phi_n-V(\phi_{n-1}+\phi_{n+1})-\frac{\chi^2}{\kappa}\,(2|\phi_n|^2+|\phi_{n+1}|^2+|\phi_{n-1}|^2)\phi_n+\frac{\chi^2}{\kappa}\left\{\sum_{m=1}^{N}\int_0^t ds\; M_{n-m}(t-s)\times\left[\frac{d}{ds}\,|\phi_m(s)|^2\right]\phi_n+\sum_{m=1}^{N} M_{n-m}(t)|\phi_m(0)|^2\right\}+\frac{\chi^2}{\kappa}\,[f_{n+1}(t)-f_{n-1}(t)]\phi_n. \tag{38}$$

Equation (38) depends parametrically on time and it is immediate to see that, apart from the Langevin terms, it is equivalent to the proposed equations (28) and (29). These equations correspond to a Born-Oppenheimer (BO) approximation in which the motion of the nuclei is neglected when determining the states of the electron. In this case the lattice sites play the role of the nuclei and the amide I vibration plays the role of the electron. Just as the BO approximation is justified by different time scales of the motion of the nuclei and electrons, Eqs. (28) and (29) are justified by the ratio between the energy of the amide I vibration, around 1660 cm^{-1}, and the energy of the phonon modes, whose highest mode is $\hbar 2\sqrt{\kappa/M}$, which with the values that characterize the protein α helices is approximately 20 times smaller.

Equations (28) and (29) also satisfy both the quantum statistics of the amide I vibration and the classical statistics of the lattice motion, namely, they sample the same statistical ensemble as expressions (15)–(19). Indeed, for a given quantum state φ_n, $n=1,\ldots,N$, Eq. (29) leads to a motion of the lattice that satisfies the distribution $e^{-\beta(H_{\mathrm{ph}}+\langle\psi|H_{\mathrm{int}}|\psi\rangle)}$, which is the classical distribution for the lattice sites, corresponding to the motion of a harmonic lattice subjected to the driving forces produced by the quantum excitation. On the other hand, Eq. (28) guarantees that only eigenstates of the quantum excitation are considered and the use of the Metropolis sampling with the distribution $e^{-\beta E}$ ensures that the states of the quantum particle are taken with the correct statistical weights. The redundancy in the use of the interaction Hamiltonian is only apparent, as the BO approximation leads to a separation of variables so that $\{u_j\}$ and $\{\varphi_j\}$ each satisfies its own distribution.

In Fig. 2 the evolution, at three temperatures, of the exact-minimum-energy one-quantum state for the values of the parameters used is displayed. The coupling to the thermal bath is such that stochastic forces are applied to all sites at every 0.05 ps. This allows for a clear view of the mechanism of decay of the initial soliton state. Without the bath, the excitation would not move because the initial condition is an exact stationary state of the system. Figure 2 shows that the coupling to the thermal bath leads to two sources of motion for the quantum excitation. At very low temperatures, when the energy gap between the minimum energy state and the next energy level is smaller than k_BT, the initial effect of the thermal bath is to kick the lattice, setting the distortion in motion and thereby dragging the excitation with it. For $T<1$ K the distortion associated with the excitation is visible above the thermal noise. Although strictly the motion con-

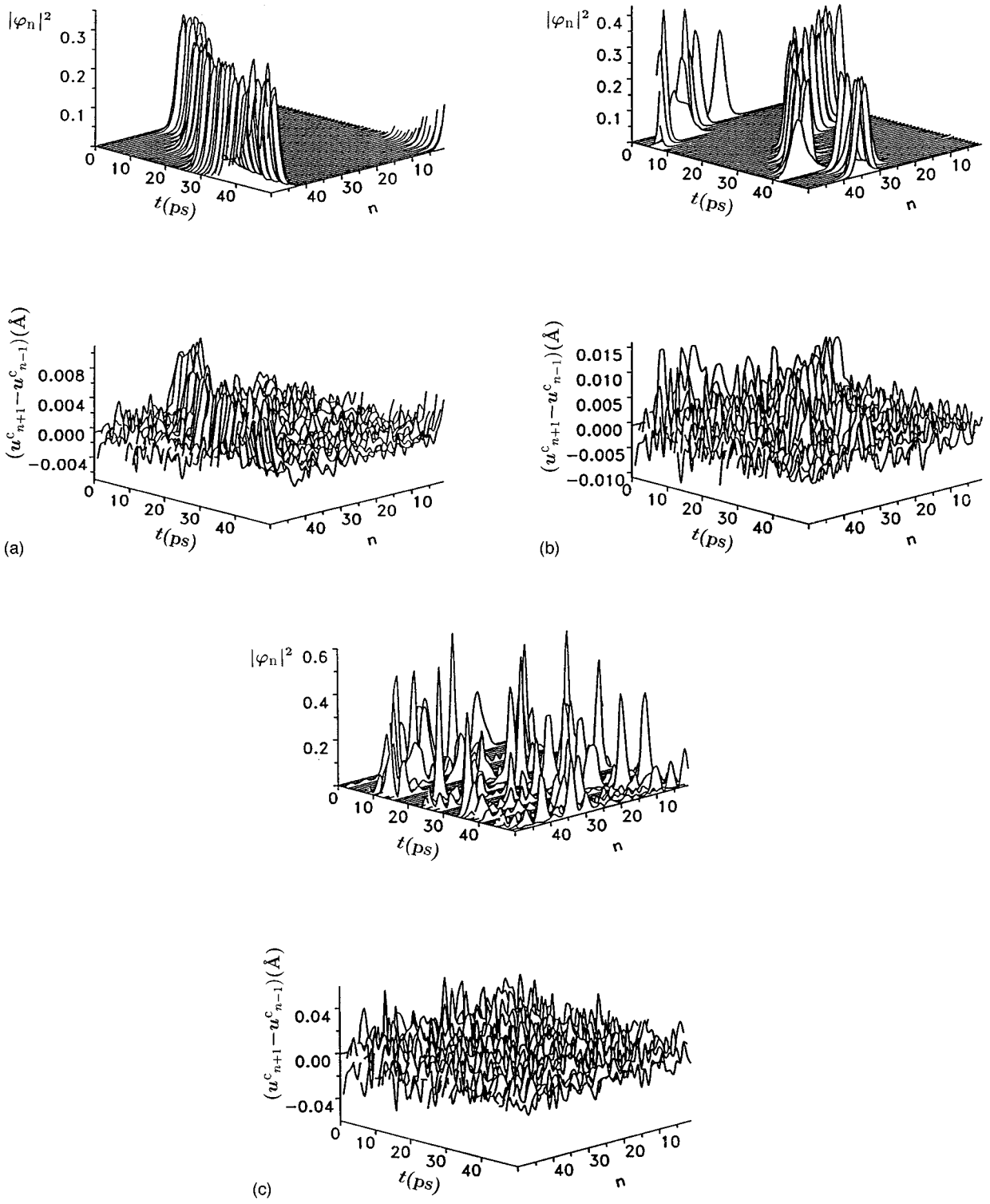

FIG. 2. Time dependence of the probability for an excitation in site n, $|\varphi_n|^2$, and its correlated lattice distortion $-(u^c_{n+1}-u^c_{n-1})$, calculated by integration of Eqs. (28) and (29). The initial condition is the exact-minimum-energy one-quantum state of the mixed quantum-classical Davydov model. The temperature is (a) $T=0.1$ K, (b) $T=0.5$ K, and (c) $T=10$ K. $M=5.7\times10^{-25}$ kg, and other parameters are as in Fig. 1. Stochastic forces and damping are applied every 0.05 ps.

sists of a scattering of the soliton by thermal phonons, the propagation in Fig. 2(a) resembles the coherent propagation that characterizes a soliton. As the temperature is increased, the thermal kicks to lattice become stronger and the motion of the distortion and, consequently, the motion of the excitation are faster, as shown in Fig. 2(b). When k_BT becomes larger than the energy gap between adjacent levels, higher levels than the minimum are also populated. These quantum transitions are associated with physical jumps of the excitation from one site to another. Figure 2(b) shows such a process occurring 40 ps into the simulation. In Fig. 2(b), the excitation that jumped due to a quantum transition is able to

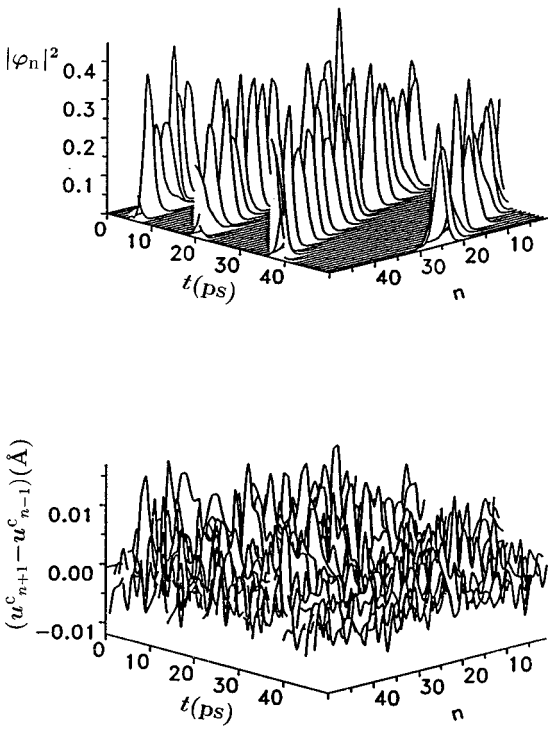

FIG. 3. Time dependence of the probability for an excitation in site n, $|\varphi_n|^2$, and its correlated lattice distortion $-(u^c_{n+1}-u^c_{n-1})$. The initial condition is the same as in Fig. 2 and the temperature is 10 K. A weaker coupling to the thermal bath than in Fig. 2 is considered, with the stochastic forces and damping terms applied to one site at a time every 0.2 ps. Other parameters are as in Fig. 2.

induce a distortion at the new site because, at $T=0.5$ K, the distortion due to thermal agitation is smaller than that induced by the presence of the excitation. As the temperature increases, the distortion induced by the excitation becomes smaller than that induced by thermal agitation and the lattice disorder is essentially thermal, as seen in Fig. 2(c). The two sources of motion thus lead to a Brownian-like motion of a very localized excitation in a noisy lattice, as was observed previously at biological temperatures [9,10]. This is different from the predictions of the classical Langevin simulations [19], according to which not only is the lattice essentially disordered but also the excitation becomes dispersed at biological temperatures.

Figure 3 illustrates another problem associated with the determination of thermal lifetimes. It shows the result of integrating Eqs. (28) and (29) with a weaker coupling to the thermal bath in which the stochastic forces are applied every 0.2 ps and to one site at a time, with inhibition of quantum transitions. In this case, at 10 K, the same temperature as in Fig. 2(c), it is possible to find ''coherent,'' solitonlike, propagation of the excitation, lasting at least 50 ps. In practice, very little is known about the nature of the bath in these systems and thus it is not possible to eliminate this arbitrariness in the estimation of soliton lifetimes.

VII. DISCUSSION

In Secs. II–IV the equilibrium regimes of the full quantum, the mixed quantum-classical, and the classical Davydov systems were considered. The aim is threefold. First, we want to define the exact equilibrium behavior of the amide I in the three systems. While the nonequilibrium regime remains obscure in many cases, it is possible to define the equilibrium properties with great accuracy. This allows us to use the equilibrium averages of the quantum Davydov system to evaluate the validity of the mixed quantum-classical and of the classical regimes. The equilibrium studies of the full quantum Davydov system show that at low temperature the amide I vibration occupies about five sites and correlated with its position there is a lattice contraction [11]. Although this state does not coincide with the solution(s) proposed by Davydov [1] and studied by many other authors [2–4], it possesses the same essential features and can be legitimately be called *the* Davydov soliton [27]. The mixed quantum classical system also leads to a soliton, at low temperature, but one for which the lattice contraction is *smaller* than that of the full quantum system [14] and the full classical system leads to the same states as the mixed quantum-classical system (with the provisos made in Sec. VI). At finite temperature, both the mixed quantum-classical and the full quantum systems lead to a localized amide I excitation. Although this state preserves one of the features of the Davydov soliton it does not coincide with it because the lattice contraction associated with the position of the amide I vibration is much smaller than the distortions induced by thermal agitation.

A second aim is to use the full quantum system as a standard and compare the results of the mixed quantum-classical and the classical systems to that standard. While the classical system does not approach the quantum system either at low or at high temperature, the mixed quantum-classical differs from the quantum system at very low temperature but becomes very approximate to the full quantum system at biological temperatures. Our results are thus in agreement with those of other authors [5,28] in that at low temperatures the mixed quantum-classical system can be different from the quantum system. However, our results also indicate that these differences decrease as the temperature increases and are negligible at biological temperatures. A first-order approximation for the average of a general quantity $\hat{B}$ leads to a critical temperature of 60 K, above which the results of the mixed quantum-classical and the full quantum become very similar (see Sec. III). A direct comparison of the lattice contraction for the two systems suggest a value of 11 K for the critical temperature [14]. The results in Secs. II and III confirm the appropriateness of the mixed quantum-classical system to describe the states of the amide I vibration in a protein at biological temperatures.

The third aim of studying the equilibrium behavior is that, as emphasized in the Introduction, the equilibrium properties of a system constitute a very important reference point for the nonequilibrium studies. Having assessed the validity of the mixed quantum-classical regime, we would like to devise equations of motion for the nonequilibrium situation in that regime for which the quantum statistics of the amide I excitations are obeyed. Equations (28) and (29) are proposed with those aspects in mind. We have shown that they correspond to a BO-like approximation, whose validity is set by the ratio between the frequency of the quantum particle with respect to the frequency of the classical phonons. They also satisfy both the quantum statistics for the excitation and the

classical statistics for the lattice. Equations (28) and (29) thus follow the criterion of leading to the same results as the equilibrium averages in the limit of a long simulation. It should also be pointed out that they can be easily extended to study of the finite-temperature properties of other systems in which general quantum quasiparticles interact with classical oscillators and for which relation (37) is satisfied.

Equations (28) and (29) predict that, at biological temperatures, a localized amide I vibration will hop from site to site in a Brownian-like manner. Although Davydov concentrated on the application of his model to muscle contraction (and the limitations of the Davydov model in that respect have been emphasized previously [10]), ATP is used as a fuel in many other biological processes and the stochastic mechanism for energy transfer in proteins predicted by Eqs. (28) and (29) may constitute the first step in many of those processes. According to Eqs. (28) and (29) the initial local excitation created by the hydrolysis of ATP can travel to any other region of the protein in the picosecond time scale. The Davydov model does not describe how this initial excitation is then transformed into the more classical motions associated with conformational changes. This constitutes a whole other field of research.

The Davydov system has been the object of many theoretical studies. In many cases, although the starting point is the full quantum case, the approximations made effectively place the work either in the mixed quantum-classical case or in the full classical case. Some of the investigations involve different approximations made within the full quantum Davydov system that do not lead to any particular regime and whose degree of approximation is difficult to quantify. On the other hand, other, contradictory, claims made by different authors should be considered in the light of the differences between the regimes (see, e.g., [2] and references therein).

A very important task at present is to devise and perform experimental tests on the basic assumption of the Davydov model, namely, that the initial carrier of the energy released in the hydrolysis of ATP is the amide I vibration. Until now, the applicability of the Davydov Hamiltonian has only had indirect confirmation in acetanilide [2,29], an organic crystal that has the same hydrogen-bonded chains as α helices. More recently, other experiments have been suggested [30]. It is with the purpose of stimulating similar experimental work directly on proteins that a measurable quantity, namely, the absorption spectrum associated with the amide I excitation, is plotted in Fig. 1. The experimental verification of these and other quantities is being pursued.

Finally, this study does not address the question of the validity of the Davydov model itself and simply derives the consequences in each regime. A more fundamental question are the limitations of the Davydov model itself. It has been pointed out by Takeno and others [31] that the Davydov model does not provide a very adequate description of vibrational states and that extra terms should be included in the Hamiltonian, which break the conservation of the amide I excitation. Such an extension of the Davydov model is being investigated.

ACKNOWLEDGMENTS

This work was supported by the BBSRC through Grant No. B/93/AF/1646 and through funding for supercomputing facilities. A BBSRC ISIS travel grant for L.C.H. is also acknowledged.

APPENDIX A: DERIVATION OF EQ. (11)

We follow the path-integral approach first proposed by Feynman [12] and subdivide the path from q^0 to q^{2L} in L intervals, numbered by the even numbers from 0 to $2L$ for reasons that will become apparent below. The numerator of the thermodynamic average (10) thus becomes

$$\begin{aligned}\int \cdots \int \prod_{j=1,N}^{N} (dq_j^0 dq_j^2 \cdots dq_j^{2L-2} dq_j^{2L} \equiv dq_j^0) \\ \times \sum_{n_0,n_2,\ldots,n_{2L}\equiv n_0=1} \langle \psi_{n_0} | \langle Q_j^0 | e^{-\tau \hat{H}} | Q_j^2 \rangle | \psi_{n_2} \rangle \\ \times \langle \psi_{n_2} | \langle Q_j^2 | e^{-\tau \hat{H}} | Q_j^4 \rangle | \psi_{n_4} \rangle \times \cdots \times \\ \times \langle \psi_{n_{2L-4}} | \langle Q_j^{2L-4} | e^{-\tau \hat{H}} | Q_j^{2L-2} \rangle | \psi_{n_{2L-2}} \rangle \\ \times \langle \psi_{n_{2L-2}} | \langle Q_j^{2L-2} | \hat{B} | Q_j^{2L} \rangle | \psi_{n_{2L}} \rangle . \end{aligned} \tag{A1}$$

Notice that expression (A1) is exact, as it just corresponds to inserting L partitions of unity $|Q\rangle\langle Q|$ in the L factors of the expression $e^{-\tau \hat{H}} \cdots e^{-\tau \hat{H}}$, with $\tau = \beta/L$. In order to determine the matrix elements $\langle \psi_{n_s} | \langle Q_j^s | e^{-\tau \hat{H}} | Q_j^{s+2} \rangle | \psi_{n_{s+2}} \rangle$, $s = 1, \ldots, 2L$, we make the first and only approximation by using the Trotter formula

$$e^{-\tau \hat{H}} = e^{-\tau \hat{H}_0} e^{-\tau \hat{H}_1}, \tag{A2}$$

which is rigorously true when $\hat{H}_0$ commutes with $\hat{H}_1$. In this case we have

$$\hat{H}_0 = \frac{1}{2M} \sum_{j=1}^{N} \hat{P}_i^2, \tag{A3}$$

$$\hat{H}_1 = \hat{H}_{\rm qp} + \hat{H}_{\rm int} + \tfrac{1}{2} \kappa \sum_{j=1}^{N} (\hat{U}_j - \hat{U}_{j-1})^2, \tag{A4}$$

and the Trotter formula is valid to order τ^2. As $L \to \infty$ the quantum-mechanical expressions below become exact. In practice L is chosen large enough for the error involved in the Trotter formula to be negligible. Using the Trotter formula and inserting another L partitions of unity in Eq. (A2) the numerator of Eq. (10) becomes

$$\begin{aligned}\int \cdots \int \prod_{j=1,N}^{N} (dq_j^0 dq_j^1 dq_j^2 \cdots dq_j^{2L} \equiv dq_j^0) \\ \times \sum_{n_0,n_1,n_2,\ldots,n_{2L},n_{2L}\equiv n_0=1} \langle \psi_{n_0} | \langle Q_j^0 | e^{-\tau \hat{H}_0} | Q_j^1 \rangle | \psi_{n_1} \rangle \\ \times \langle \psi_{n_1} | \langle Q_j^1 | e^{-\tau \hat{H}_1} | Q_j^2 \rangle | \psi_{n_2} \rangle \langle \psi_{n_2} | \langle Q_j^2 | e^{-\tau \hat{H}_0} | Q_j^3 \rangle | \psi_{n_3} \rangle \\ \times \langle \psi_{n_3} | \langle Q_j^3 | e^{-\tau \hat{H}_1} | Q_j^4 \rangle | \psi_{n_4} \rangle \times \cdots \times \\ \times \langle \psi_{n_{2L-2}} | \langle Q_j^{2L-2} | e^{-\tau \hat{H}_0} | Q_j^{2L-1} \rangle | \psi_{n_{2L-1}} \rangle \\ \times \langle \psi_{n_{2L-1}} | \langle Q_j^{2L-1} | e^{-\tau \hat{H}_1} \hat{B} | Q_j^{2L} \rangle | \psi_{n_{2L}} \rangle . \end{aligned} \tag{A5}$$

We can now evaluate the matrix elements

$$\langle\psi_{n_{2s}}|\langle Q_j^{2s}|e^{-\tau\hat{H}_0}|Q_j^{2s+1}\rangle|\psi_{n_{2s+1}}\rangle=\rho_j(2s,2s+1;\tau)\times\langle\psi_{n_{2s}}|\psi_{n_{2s+1}}\rangle \tag{A6}$$

$$\begin{aligned}&\langle\psi_{n_{2s+1}}|\langle Q_j^{2s+1}|e^{-\tau\hat{H}_1}|Q_j^{2s+2}\rangle|\psi_{n_{2s+2}}\rangle\\&=\langle\psi_{n_{2s+1}}|e^{\tau\hat{H}_1(\{q_j^{2s+2}\})}|\psi_{n_{2s+2}}\rangle\,\delta(\{(q_j^{2s+2}-q_j^{2s+1})\})\\&=e^{-\tau E_{n_{2s+2}}}\langle\psi_{n_{2s+1}}|\psi_{n_{2s+2}}\rangle\,\delta(\{(q_j^{2s+2}-q_j^{2s+1})\}),\end{aligned} \tag{A7}$$

$$[\hat{H}_{\rm qp}+\tilde{H}_{\rm int}(\{q_j^{2s+2}\})]|\psi_{n_{2s+2}}\rangle=E_{n_{2s+2}}|\psi_{n_{2s+2}}\rangle, \tag{A8}$$

where $\rho_j(2s,2s+1;\tau)$ is the density matrix of a free particle [12],

$$\rho_j(2s,2s+1;\tau)=\left(\frac{L}{2\pi\lambda^2}\right)^{3/2}\exp\left[-\frac{L}{2\lambda^2}\,(q_j^{2s+1}-q_j^{2s})^2\right], \tag{A9}$$

$$\lambda^2=\hbar^2\tau/M. \tag{A10}$$

Substituting Eqs. (A6)–(A8) into Eq. (A5) and after some algebra, the expression for the thermodynamic average (11)–(14) is obtained.

APPENDIX B: DERIVATION OF EQ. (30)

Equation (30) can be obtained by first introducing the Laplace transforms of $u_n\equiv u_n(t)$ and $|\varphi_n(t)|^2\equiv\xi_n(t)$, respectively,

$$v_n(s)=\int_0^\infty \exp(-st)u_n(t)dt,$$
$$\zeta_n(s)=\int_0^\infty \exp(-st)\xi_n(t)dt \tag{B1}$$

to reduce Eq. (27) to

$$s^2v_n(s)-\frac{\kappa}{M}\,[v_{n+1}(s)+v_{n-1}(s)-2v_n(s)]=su_n(0)+\dot{u}_n(0)+\frac{\chi}{M}\,[\zeta_{n+1}(s)-\zeta_{n-1}(s)]. \tag{B2}$$

Introducing the Fourier transforms of $v_n(s)$, $\zeta_n(s)$, $u_n(t)$, $\dot{u}_n(t)$, and $\xi_n(t)$,

$$v_k(s)=\frac{1}{N}\sum_n e^{-\iota kn}v_n(s),\quad \zeta_k(s)=\frac{1}{N}\sum_n e^{-\iota kn}\zeta_n(s),$$
$$u_k(t)=\frac{1}{N}\sum_n e^{-\iota kn}u_n(t),\quad \dot{u}_k(t)=\frac{1}{N}\sum_n e^{-\iota kn}\dot{u}_n(t),$$
$$\xi_k(s)=\frac{1}{N}\sum_n e^{-\iota kn}\xi_n(s), \tag{B3}$$

in Eq. (B2), we obtain

$$v_k(s)=\frac{s}{s^2+\omega^2(k)}\,u_k(0)+\frac{1}{s^2+\omega^2(k)}\,\dot{u}_k(0)+\frac{\chi}{M}\,\frac{2\iota\,\sin(k)}{s^2+\omega^2(k)}\,\zeta_k(s), \tag{B4}$$

where

$$\omega^2(k)=2\,\frac{\kappa}{M}\,[1-\cos(k)] \tag{B5}$$

is the square of the eigenfrequency of acoustic phonons described by Eq. (27) with $\chi=0$. Our objective here is to obtain an exact formal expression for $u_{n+1}-u_{n-1}$, which appears on the right-hand side of Eq. (27). For this purpose, we multiply by the factor $2\iota\,\sin(k)$ both sides of Eq. (B4) and then rearrange terms to obtain

$$\begin{aligned}2\iota\,\sin(k)v_k(s)=&-\frac{2\chi}{\kappa}\,[1+\cos(k)]\zeta_k(s)\\&+\frac{2\chi}{\kappa}\,[1+\cos(k)]\,\frac{s}{s^2+\omega^2(k)}\\&\times[s\zeta_k(s)-\xi_k(0)]+\frac{2\chi}{\kappa}\,[1+\cos(k)]\\&\times\frac{s}{s^2+\omega^2(k)}\,\xi_k(0)+2\iota\,\sin(k)\\&\times\left[\frac{s}{s^2+\omega^2(k)}\,u_k(0)+\frac{1}{s^2+\omega^2(k)}\,\dot{u}_k(0)\right].\end{aligned} \tag{B6}$$

Taking the inverse Laplace transform of Eq. (B6) gives

$$\begin{aligned}2\iota\,\sin(k)u_k(t)=&-\frac{2\chi}{\kappa}\,[1+\cos(k)]\xi_k(t)\\&+\frac{2\chi}{\kappa}\,[1+\cos(k)]\\&\times\int_0^t\cos[\omega(k)(t-\tau)]\dot{\xi}_k(\tau)d\tau\\&+\frac{2\chi}{\kappa}\,[1+\cos(k)]\cos[\omega(k)t]\xi_k(0)\\&+2\iota\,\sin(k)\left\{\cos[\omega(k)t]u_k(0)\right.\\&\left.+\frac{\sin[\omega(k)t]}{\omega(k)}\,\dot{u}_k(0)\right\}.\end{aligned} \tag{B7}$$

Then, performing an inverse Fourier transform on Eq. (B7) we arrive at the result

$$u_{n+1}-u_{n-1}=-\frac{\chi}{\kappa}[2\xi_n(t)+\xi_{n+1}(t)+\xi_{n-1}(t)]$$
$$+\frac{\chi}{\kappa}\sum_m\int_0^t d\tau[2C_{n-m}(t-\tau)$$
$$+C_{n+1-m}(t-\tau)+C_{n-1-m}(t-\tau)]\dot{\xi}_m(\tau)$$
$$+\frac{\chi}{\kappa}\sum_m[2C_{n-m}(t)+C_{n+1-m}(t)$$
$$+C_{n-1-m}(t)]\xi_m(0)+f_{n+11}-f_{n-1}, \quad \text{(B8)}$$

where

$$C_n(t)=\frac{1}{N}\sum_k \cos[\omega(k)t]e^{\iota kn}, \quad \text{(B9)}$$

$$f_n(t)=\frac{1}{N}\sum_k\left\{\cos[\omega(k)t]u_k(0)+\frac{\sin[\omega(k)t]}{\omega(k)}\dot{u}_k(0)\right\}e^{\iota kn}. \quad \text{(B10)}$$

Taking the limit $N\to\infty$ and replacing the sums by integrals in Eqs. (B9) and (B10), we can write the quantities $C_n(t)$ and $f_n(t)$ in terms of Bessel functions as

$$C_n(t)=J_{2n}(\omega_1 t), \quad \text{(B11)}$$

$$f_n(t)=\sum_m[J_{2(n-m)}(\omega_1 t)u_m(0)+J^*_{2(n-m)}(\omega_1 t)\dot{u}_m(0)], \quad \text{(B12)}$$

where

$$\omega_1^2=4\frac{\kappa}{M}, \quad J_n^*(x)=\int J_n(x)dx. \quad \text{(B13)}$$

Then, in terms of

$$M_n(t)=2J_{2n}(\omega_1 t)+J_{2(n+1)}(\omega_1 t)+J_{2(n-1)}(\omega_1 t), \quad \text{(B14)}$$

Eq. (B8) takes the form given by Eq. (30).

[1] A. S. Davydov, J. Theor. Biol. **38**, 559 (1973); **66**, 379 (1977); Int. J. Quantum Chem. **16**, 5 (1979); *Biology and Quantum Mechanics* (Pergamon, New York, 1982); Physica D **3**, 1 (1981); Usp. Fiz. Nauk **138**, 603 (1982) [Sov. Phys. Usp. **25**, 898 (1982)]; L. S. Brizhik and A. S. Davydov, Phys. Status Solidi B **115**, 615 (1983).

[2] A. Scott, Phys. Rep. **217**, 1 (1992).

[3] D. Kapor, M. Skrinjar, Z. Ivic, and Z. Przulj, Bioelectrochem. Bioenerg. **41**, 93 (1996); Z. Ivic, Z. Przulj, D. Kapor, and M. Skrinjar, *ibid.* **41**, 43 (1996); Z. Ivic, Z. Przulj, D. Kostic, D. Kapor, and M. Skrinjar, Phys. Rev. B **54**, 2992 (1996).

[4] W. Förner, J. Mol. Model. **2**, 70 (1996); **2**, 103 (1996); Phys. Rev. B **53**, 6291 (1996).

[5] V. M. Kenkre, S. Raghavan, A. R. Bishop, and M. I. Salkola, Phys. Rev. B **53**, 5407 (1996); S. Raghavan, V. M. Kenkre, A. R. Bishop, and M. I. Salkola, *ibid.* **53**, 8457 (1996).

[6] A. V. Zolotariuk, K. H. Spatschek, and A. V. Savin, Phys. Rev. B **54**, 266 (1996); Europhys. Lett. **31**, 531 (1995).

[7] M. Daniel and K. Deepamala, Physica A **221**, 241 (1995); E. A. Bartnik, J. A. Tuszynski, and D. Sept, Phys. Lett. A **204**, 263 (1995); D. Todorovic, L. Ristovski, and B. S. Tosic, Phys. Status Solidi B **190**, 251 (1995); H. Rosu, Nuovo Cimento D **18**, 477 (1996).

[8] There are several ways of quantizing systems. Here we consider the following way: The quantum correspondent of a classical displacement u, the classical momentum p, and the classical complex amplitude $a\propto x+ip$ are, respectively, the displacement operator $\hat{U}$, the quantum momentum operator $\hat{P}$, and the annihilation operator $\hat{A}$.

[9] L. Cruzeiro-Hansson, Europhys. Lett. **33**, 655 (1996).

[10] L. Cruzeiro-Hansson, Phys. Lett. A **223**, 383 (1996).

[11] X. Wang, D. W. Brown, and K. Lindenberg, Phys. Rev. Lett. **62**, 1796 (1989); in *Davydov's Soliton Revisited*, edited by P. L. Christiansen and A. C. Scott (Plenum, New York, 1990).

[12] R. P. Feynman, *Statistical Mechanics* (Benjamin, Reading, MA, 1972).

[13] N. Metropolis, A. W. Rosenbluth, M. N. Rosenbluth, A. H. Teller, and E. Teller, J. Chem. Phys. **21**, 1087 (1953).

[14] L. Cruzeiro-Hansson and V. M. Kenkre, Phys. Lett. A **203**, 362 (1995).

[15] L. Cruzeiro-Hansson, Phys. Rev. A **45**, 4111 (1992).

[16] J. M. Hyman, D. W. McLaughlin, and A. C. Scott, Physica D **3**, 23 (1981); A. C. Scott, Phys. Scr. **29**, 279 (1984); L. MacNeil and A. C. Scott, *ibid.* **29**, 284 (1981).

[17] G. P. Tsironis and V. M. Kenkre, Phys. Lett. A **127**, 209 (1988); V. M. Kenkre and H.-L. Wu, *ibid.* **135**, 120 (1989).

[18] P. W. Miloni, J. R. Ackerhalt, and H. R. Galbraith, Phys. Rev. Lett. **50**, 966 (1983); D. Feinberg and J. Ranninger, Physica D **14**, 29 (1984).

[19] P. S. Lomdahl and W. C. Kerr, Phys. Rev. Lett. **55**, 1235 (1985).

[20] S. Nosé, Mol. Phys. **52**, 255 (1984); W. G. Hoover, Phys. Rev. A **31**, 1695 (1985); S. Nosé, Prog. Theor. Phys. Suppl. **103**, 1 (1991).

[21] W. Förner, J. Phys. Condens. Matter **3**, 3235 (1991); **3**, 4333 (1991); Phys. Rev. A **44**, 2694 (1991); J. Phys. Condens. Matter **4**, 1915 (1992); J. Comput. Chem. **13**, 275 (1992); J. Phys. Condens. Matter **5**, 803 (1993); **5**, 823 (1993); **5**, 3883 (1993); **5**, 3897 (1993).

[22] L. Cruzeiro-Hansson, V. A. Okhonin, R. G. Khlebopros, and I. N. Yassievich, Nanobiology **1**, 395 (1992).

[23] F. Mauri, R. Car, and E. Tosatti, Europhys. Lett. **24**, 431 (1993).

[24] V. M. Kenkre and P. Grigolini, Z. Phys. B **90**, 247 (1993).

[25] L. Cruzeiro-Hansson, Physica D **68**, 65 (1993).

[26] J. C. Eilbeck, P. S. Lomdahl, and A. C. Scott, Physica D **16**, 318 (1985); A. C. Scott, E. Gratton, E. Shyamsunder, and G. Careri, Phys. Rev. B **32**, 5551 (1985).

[27] The soliton state referred to *is* described by a translationally invariant wave function that is characterized by an equal probability for the amide I to be in each of the sites. However, the

measurement of any quantity involves the collapse of the wave function and a break of the translational symmetry. Notice also that the mixed quantum-classical wave function (25), which takes the displacements and momenta as parameters, already implies a break of translational symmetry and is in fact a correlation, i.e., φ_n is the probability amplitude for an excitation in site n when the particular lattice conformation is represented by $\{u_n\}$. Comparisons between regimes should be made by comparing measurable quantities.

[28] L. Bonci, P. Grigolini, and D. Vitali, Phys. Rev. A **42**, 4452 (1990); D. Vitali, L. Bonci, R. Mannella, and P. Grigolini, *ibid.* **45**, 2285 (1992); L. Bonci, and P. Grigolini, *ibid.* **46**, 4445 (1992).

[29] G. Careri, U. Buontempo, F. Carta, E. Gratton, and A. C. Scott, Phys. Rev. Lett. **51**, 304 (1983); J. C. Eilbeck, P. S. Lomdahl, and A. C. Scott, Phys. Rev. B **30**, 4703 (1984); G. Careri, U. Buontempo, F. Galluzzi, A. C. Scott, E. Gratton, and E. Shyamsunder, *ibid.* **30**, 4689 (1984); G. Careri, E. Gratton, and E. Shyamsunder, Phys. Rev. A **37**, 4048 (1988).

[30] W. Fann, L. Rothberg, M. Robertson, S. Benson, J. Madey, S. Etemad, and R. Austin, Phys. Rev. Lett. **64**, 607 (1990); T. Rozgonyi, and A. Lörincz, J. Appl. Phys. **75**, 1861 (1994).

[31] S. Takeno, Prog. Theor. Phys. **69**, 1798 (1983); **71**, 395 (1984); **73**, 853 (1985); in *Computer Analysis for Life Science*, edited by C. Kawabata and A. R. Bishop (Ohmsha, Tokyo, 1985), p. 47; Prog. Theor. Phys. **75**, 1 (1986); J. Phys. Soc. Jpn. **58**, 1639 (1989); **59**, 3127 (1990); X. Wang, D. W. Brown, and K. Lindenberg, Phys. Rev. B **39**, 5366 (1989).